Performance of Spur Gears Considering Surface Roughness and Shear Thinning Lubricant

S. Akbarzadeh

M. M. Khonsari[1]
e-mail: Khonsari@me.lsu.edu

Department of Mechanical Engineering,
Louisiana State University,
2508 CEBA,
Baton Rouge, LA 70803

*A model is developed for predicting the performance of spur gears with provision for surface roughness. For each point along the line of action, the contact of pinion and gear is replaced by that of two cylinders. The radii of cylinders, transmitted load, and contact stress are calculated, and lubricant film thickness is obtained using the load-sharing concept of Johnson et al. (1972, "A Simple Theory of Asperity Contact in Elastohydrodynamic Lubrication," Wear, **19**, pp. 91–108) To validate the analysis, the predicted film thickness and the friction coefficient are compared to published theoretical and experimental data. The model is capable of predicting the performance of gears with non-Newtonian lubricants—such as that of shear thinning lubricants—often used in gears. For this purpose, a correction factor for shear thinning film thickness introduced by Bair (2005, "Shear Thinning Correction for Rolling/Sliding Electrohydrodynamic Film Thickness," Proc. Inst. Mech. Eng., Part J: J. Eng. Tribol., **219**, pp. 1–6) has been employed. The results of a series of simulations presenting the effect of surface roughness on the friction coefficient are presented and discussed. The results help to establish the lubrication regime along the line of action of spur gears.* [DOI: 10.1115/1.2805431]

Keywords: gear, film thickness, line of action, friction coefficient, surface roughness, shear thinning lubricant

1 Introduction

Gears are used to transmit force between two parts of the same machine or between two devices, often with a mechanical advantage that allows increasing or decreasing the rotational speed or torque from one shaft to another. Study of gears embodies almost all aspects of tribology. As is commonly the case in the analysis of most tribological components, the key parameters of interest in gears are the lubricant film thickness, the dimensionless film parameter Λ, and the coefficient of friction. The first two parameters are important in terms of reliability and damage, while the third parameter is a measure of the efficiency of the gear set in terms of the required power.

It is well known that lubrication regime in gears is governed by mixed or partial elastohydrodynamic lubrication (EHL) regimes—a subject that has captured the attention of many researchers over the past four decades. Gear surfaces are typically much rougher than those of shaft/bushing surfaces, making it necessary to take surface roughness into consideration. Johnson et al. [1] proposed a theory of asperity contact in EHL. They combined the Greenwood–Williamson model of rough surfaces with EHL theory and introduced the load-sharing concept. Later, Patir and Cheng [2] solved the average Reynolds equation for rough surfaces. They studied both isotropic surfaces and surfaces with directional patterns. Lee [3] proposed an analytical model and conducted some experiments on the scuffing of rollers under EHL. Hua and Khonsari [4] solved the transient EHL equation in spur gears, assuming that the surfaces are smooth. Chang [5] proposed a model for partial EHL and considered the asperities to be frictionless. Later, Flodin and Andersson [6] studied wear in spur and helical gears, assuming dry contact. Chapkov et al. [7] have recently proposed a model to predict roughness amplitude reduction in both Newtonian and non-Newtonian EHL contacts. Their model includes the influence of surface roughness wavelength and contact operating conditions and predicts the deformed shape. They showed that surfaces with short wavelength will slightly deform, and therefore there is a high probability of asperity contact. Surfaces with longer wavelength, on the other hand, will be deformed more, and therefore less asperity contact will occur. The majority of pure mineral oils of similar molecular size exhibit Newtonian behavior, where their viscosities are independent of shear rate. Nevertheless, there are practical applications where the lubricant's viscosity varies with the rate of shear. For example, the so-called shear thinning lubricants experience a drop with increasing shear rate [8]. An excellent experimental application of shear fluids for lubrication of two cylindrical rollers is reported by Dyson and Wilson [9]. They showed that their reported measurement of film thickness is significantly lower than what the well-established EHL film thickness formula predicts. Bair and Khonsari [10] showed that some gear oils show a shear thinning behavior and compared the analytical and experimental flow curve. Since shear thinning lubricants are becoming more popular in some industrial applications, their behavior is studied in this research. To account for shear thinning effect, Bair [11] recently proposed a correction factor for predicting the film thickness in an EHL line contact in the form of $\phi = h_N / h_{NN}$, where h_N is the Newtonian film thickness and h_{NN} is the actual film thickness for the lubricant. The expression for ϕ is a function of the slide to roll ratio, lubricant properties, velocity, and power-law exponent.

In this paper, we apply the load-sharing concept of Johnson et al. to predict the performance of a spur gear. The surface properties are amongst the inputs to the model, which is capable of taking shear thinning effect into consideration. Once the values of film thickness along the line of action (LoA) are obtained, the fluid friction force and hence the friction coefficient can be easily predicted.

2 Model

One of the most important issues in gear sets is the friction coefficient. The aim of this research is to present a model that

[1]Corresponding author.

Contributed by the Tribology Division of ASME for publication in the JOURNAL OF TRIBOLOGY. Manuscript received June 10, 2007; final manuscript received September 12, 2007; published online April 7, 2008. Review conducted by Benyebka Bou-Said.

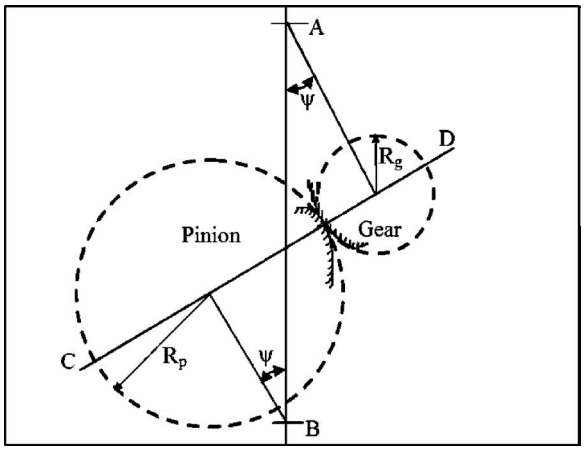

Fig. 1 Representation of pinion and gear with rollers

takes into consideration the surface properties (i.e., spectral moments of profile) and type of lubricant as well as gear geometry and the loading condition as the input and predicts the film thickness and the friction coefficient along the LoA.

Surface profiles are described either by spectral moments (m_0, m_2, and m_4) or by determining the asperity density n, the radius of asperities β, and the rms of the surface σ. These parameters are related to the spectral moments of the surface through the following equations [12]. If $z(x)$ is the profile in an arbitrary direction x and $E[\ ]$ denotes the statistical expectations, then the zeroth, second, and fourth profile moments are

$$m_0 = E(z^2) = \sigma_s^2 \tag{1}$$

$$m_2 = E\left[\left(\frac{dz}{dx}\right)^2\right] \tag{2}$$

$$m_4 = E\left[\left(\frac{d^2z}{dx^2}\right)^2\right] \tag{3}$$

For an isotropic surface, the asperity density and the average radius of the spherical caps of the asperity can be calculated from [12]

$$\text{asperity density} = n = \frac{m_4}{6\pi\sqrt{3}m_2} \tag{4}$$

$$\text{asperity radius} = \beta = \frac{3}{8}\sqrt{\frac{\pi}{m_4}} \tag{5}$$

$$\text{surface rms} = \sigma_s = \sqrt{m_0} \tag{6}$$

If the surface is anisotropic, the values of m_2 and m_4 will vary with the direction in which the profile is taken on the surface. The maximum and minimum values for m_2 and m_4 occur in two orthogonal principal directions. The use of an equivalent isotropic surface is recommended for which m_2 and m_4 are computed as a harmonic mean of m_2 and m_4 along the principal directions.

In this model, the contact of gear teeth at each point along the LoA is represented by the contact of two cylinders having radii R_p and R_g. The radii of these cylinders vary along the LoA. Figure 1 shows how two cylinders replace the contact of pinion and gear. In this figure, ψ represents the pressure angle and CD is the line tangent to the base circles of the pinion and gear. The points of contact in spur gears are always along this line, hence commonly referred to as the LoA. The positions of contact points are determined by their coordinates, and variation of different parameters, such as the Hertzian pressure, equivalent curvature, film thickness, and friction coefficient, is evaluated along LoA.

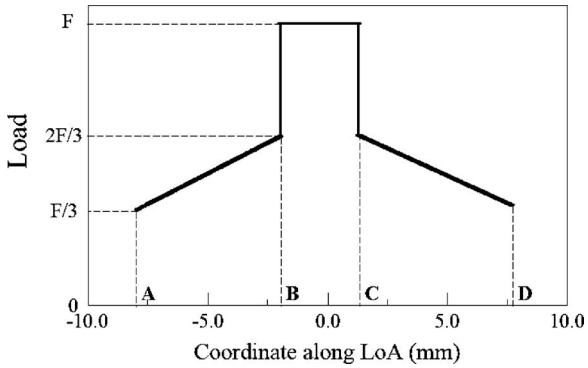

Fig. 2 Variation of load along LoA

Referring to Fig. 1, in order to analyze the pinion and gear contact, LoA is divided into several segments, and for each point on this line the radii of curvature of the pinion and gear are calculated using the following relations.

At the pitch line, the radius of curvature for the pinion is

$$\rho = \frac{d_{wp}\sin\alpha}{2} \tag{7}$$

At any other diameter, such as d_1, the radius of curvature of the pinion is

$$\rho_1 = \frac{d_1\sin\phi_1}{2} \tag{8}$$

The angle ϕ_1 can be found from the relation

$$\cos\phi_1 = \frac{d\cos\alpha}{d_1} \tag{9}$$

The radius of curvature for the gear is

$$\rho_2 = \frac{d_{wp} + d_{wg}}{2}\sin\alpha - \rho_1 \tag{10}$$

In spur gears, the load carried by each tooth varies along LoA since the number of teeth in contact changes along this line. This variation of load is shown in Fig. 2. In the derivation of this plot, it was assumed that the gear tooth stiffness changes along the tooth profile. Under this condition, it cannot be assumed that the load is equally shared among the pairs of teeth in contact since it is a statically indeterminate case [13]. This type of variation, however, does not include the effect of vibration nor does it have the effect of tooth modification. The effect of tooth modification on load distribution in gear tooth has been shown in Ref. [14]. In Fig. 2, from point *A*—i.e., the beginning of mesh—until point *B*, there are two pairs of teeth in contact, so the amount of carried load changes from one-third to two-thirds of the total load *F*. From point *B* to point *C*, however, there is only one pair of teeth in contact, and the transmitted force is equal to *F*. From point *C* to point *D*, i.e., the end of the contact, the load changes from two-thirds of *F* to one-third of *F*.

The variation of the Hertzian stress along LoA is given by the following equation:

$$P_{\text{Hertzian}} = \sqrt{\frac{F(1/R_p + 1/R_g)}{\pi B((1-\upsilon_1^2)/E_1 + (1-\upsilon_2^2)/E_2)}} \tag{11}$$

Having calculated the geometry of replacing cylinders and contact stresses, the problem now is to find the film thickness and coefficient of friction between two rollers with the known geometry and the loading condition. The analysis starts from the first point of contact and proceeds along LoA. At each point, the appropriate cylinder radii and the load are used.

The calculation of film thickness and friction coefficient for each point along LoA is based on the concept of scaling factors of Johnson et al. for the hydrodynamic part γ_1 and the asperity contact part γ_2. That is, the transmitted force F_T is the sum of the load carried by the asperity F_C and the hydrodynamic load F_H,

$$F_T = F_H + F_C \tag{12}$$

$$F_T = \frac{F_T}{\gamma_1} + \frac{F_T}{\gamma_2} \tag{13}$$

In a similar fashion, the total friction force is composed of two components: the hydrodynamic friction force ($F_{f,H}$) and the asperity friction force ($F_{f,C}$),

$$F_f = F_{f,H} + F_{f,C} \tag{14}$$

The asperity friction force is determined as

$$F_{f,C} = \sum_{i=1}^{N} f_{C_i} p_{C_i} dA_{C_i} = f_C \sum_{i=1}^{N} p_{C_i} dA_{C_i} = f_C F_C \tag{15}$$

In Eq. (15), it has been assumed that all the asperities have the same coefficient of friction. Hence, the coefficient of friction is

$$f = \frac{F_f}{F_T} = \frac{F_{f,H} + f_c F_C}{F_T} \tag{16}$$

The hydrodynamic friction force for the Newtonian lubricant is calculated as

$$F_{f,H} = 2aB\mu \frac{u_{\text{sliding}}}{h_c} \tag{17}$$

In this equation, a is the Hertzian half-width of contact, B is the roller width, u is the sliding velocity, h_c is the film thickness, and μ is the lubricant viscosity at the contact pressure. In this model, the viscosity of lubricant changes with pressure according to Roeland's equation [15],

$$\log_{10}\mu + 1.2 = (\log_{10}\mu_0 + 1.2)\left(1 + \frac{P}{C}\right)^Z \tag{18}$$

In this equation, μ_0 and μ are the viscosities of lubricant at the ambient pressure and at pressure P, both in mPa s. The parameter Z is the viscosity-pressure index and for mineral oils is assumed to be 0.6, and the value of C is taken equal to 196.1 MPa.

The film thickness calculation is based on Moes' equation [16] for central film thickness,

$$H_C = [(H_{RI}^{7/3} + H_{EI}^{7/3})^{3s/7} + (H_{RP}^{-7/2} + H_{EP}^{-7/2})^{-2s/7}]^{1/s} \tag{19}$$

where

$$s = \frac{1}{5}(7 + 8e^{(-2H_{EI}/H_{RI})}) \tag{20}$$

The dimensionless parameters used are defined as follows [17]:

$$H_{RI} = 3M^{-1}$$

$$H_{EI} = 2.621M^{-1/5}$$

$$H_{RP} = 1.287L^{2/3}$$

$$H_{EP} = 1.311M^{-1/8}L^{3/4}$$

$$H_C = h_c' U_\Sigma^{-1/2} \quad h_c' = \frac{h_c}{R}$$

$$M = WU_\Sigma^{-1/2} \quad L = GU_\Sigma^{1/4}$$

$$W = \frac{F_T}{E'RB} \quad U_\Sigma = \frac{\eta_0 u}{E'R} \quad G = \alpha_{\text{EHL}} E' \tag{21}$$

According to load-sharing method of Johnson et al., a portion of the load equal to $(1/\gamma_1)$ is taken by the fluid film. For calculating film thickness, the problem will be of two rollers with known geometry and Young's modulus of E'/γ_1 being pressed together with a force equal to $F_{\text{total}}/\gamma_1$. The rest of the load $(1/\gamma_2)$ is taken by asperities. Therefore, for calculating asperity contact pressure P_c, the problem will be two rollers with known geometry and Young's modulus of E'/γ_2 being pressed together by a force equal to $F_{\text{total}}/\gamma_2$. Applying the concept of scaling factor of Johnson et al. and substituting E'/γ_1 for E' and F_T/γ_1 for F_T, Moes' equation takes the following form:

$$H_C = [\gamma_1^{s/2}(H_{RI}^{7/3} + (\gamma_1)^{14/15}H_{EI}^{7/3})^{3s/7} + \gamma_1^{-s/2}(H_{RP}^{-7/2} + H_{EP}^{-7/2})^{-2s/7}]^{1/s}(\gamma_1)^{1/2} \tag{22}$$

where

$$s = \frac{1}{5}(7 + 8e^{(-2(\gamma_1)^{-2/5}H_{EI}/H_{RI})}) \tag{23}$$

Equation (22) has two unknowns: γ_1 and h_c. In order to determine both of the unknowns, another equation is needed. This equation comes from making the asperity contact pressure obtained from the Greenwood–Tripp model (Eq. (25)) equal to the curve fit (Eq. (24)) of Gelinck and Schipper [17]. Gelinck and Schipper [17] have shown that the central pressure is a good quantity to characterize the pressure distribution of a rough line contact. In order to fit functions to this pressure distribution, they introduced velocity-independent parameters $n' = nR\sqrt{\beta R}$ and $\sigma_s' = \sigma_s/R$, where n represents the number of asperities per unit area, β denotes the radius of asperities, and σ_s is the rms of surface roughness. After applying the concept of load sharing of Johnson et al., which leads to substituting E'/γ_2 for E', F_T/γ_2 for F_T, and $n\gamma_2$ for γ_2, the following equation was fitted to the central contact pressure,

$$p_c = \frac{1}{\gamma_2}\sqrt{\frac{F_T E'}{2\pi BR'}}\left[1 + \left(1.558(n\gamma_2 R\sqrt{\beta R})^{0.0337}\left(\frac{\sigma_s}{R}\right)^{-0.442} W^{0.4757}\right)^{-1.7}\right]^{-0.5882} \tag{24}$$

The Greenwood–Tripp equation for contact pressure is

$$p_c = \frac{8\sqrt{2}}{15}\pi\eta^2\beta^{1.5}\sigma^{2.5}E' F_{5/2}\left(\frac{h_c - d_d}{\sigma_s}\right) \tag{25}$$

The function $F_{5/2}$ is basically defined as

$$F_{5/2}(H) = \frac{1}{\sqrt{2\pi}}\int_H^\infty (s-H)^{5/2} e^{-s^2/2} ds \tag{26}$$

In the EHL formulation, instead of H, the difference between film thickness h_c and the distance between the mean plane through the summits and the mean plane through the heights of the surface, d_d, is used. That is,

$$F_{5/2}\left(\frac{h_c - d_d}{\sigma_s}\right) = \frac{1}{\sqrt{2\pi}}\int_{(h_c - d_d)/\sigma_s}^\infty \left(s - \frac{h_c - d_d}{\sigma_s}\right)^{5/2} e^{-s^2/2} ds \tag{27}$$

In Eq. (27), d_d is approximately $1.15\sigma_s$. To simplify the integration in Eq. (27), we will use the polynomial of Eq. (28), which is curve fitted to the $F_{5/2}$ [18],

$$F_{5/2} = \begin{cases} 4.4086 \times 10^{-5}(4 - \mathrm{H})^{6.804} & \text{for H} < 4 \\ 0 & \text{for H} > 4 \end{cases} \tag{28}$$

Therefore, making Eq. (24) equal to Eq. (25),

$$\sqrt{\frac{F_T E'}{2\pi B R'}}\frac{1}{\gamma_2}\times\left[1+\left(1.558(nR\gamma_2\sqrt{\beta R})^{0.0337}\left(\frac{\sigma_s}{R}\right)^{-0.442}W^{0.4757}\right)^{-1.7}\right]^{-0.5882}=\frac{8\sqrt{2}}{15}\pi\eta^2\beta^{1.5}\sigma^{2.5}E'F_{5/2}\left(\frac{h_c-d_d}{\sigma_s}\right) \quad (29)$$

Equation (24) is a curve fit of Eq. (25), but the latter is a function of film thickness also. So, the solution scheme is to choose an initial value for γ_1 and find the film thickness from Eq. (22), plug the film thickness in Eq. (24), and check if Eqs. (24) and (25) are close enough. If not, then a new value is chosen and the loop continues until the convergence criterion is satisfied. Satisfaction of convergence criterion means that the values chosen for γ_1 and, consequently, γ_2 are such that Eqs. (24) and (25) are close enough. This procedure is a general method and is independent of the type of lubricant. Hence, if the lubricant has a shear thinning behavior, a similar procedure is used and the calculated film thickness is corrected using the Bair's correction factor [11]. Since this correction factor ϕ is a function of the slide to roll ratio and the velocity in addition to lubricant properties, its variation along LoA should be considered. In Sec. 4, the behavior of a shear thinning lubricant is investigated.

3 Numerical Simulations Procedure

The numerical simulation procedure starts with calculating the surface properties. In other words, asperity radius, asperity density, and the rms of the surface should be known. If these parameters are not provided and instead the spectral moments of the surface are given, then Eqs. (4)–(6) will be used to calculate the surface properties from spectral moments. For each point along LoA, the radii of curvature are calculated using Eqs. (7)–(10). These radii are the radii of the replacing cylinders. Equation (11) is used to calculate the Hertzian stress between contacting cylinders along the LoA. So far, for all the points along LoA, the radii of cylinders and the contact stress are known. Then, a value for γ_1 is chosen and film thickness is calculated using Eq. (22) and nondimensional parameters of Eq. (21). Then, both sides of Eq. (29) are calculated. If the difference between right and left sides of Eq. (29) divided by the right hand side is larger than a specified tolerance error ε (e.g., 1×10^{-5}), then a new value for γ_1 is assumed, and the calculations are repeated until the convergence criteria are satisfied. Once the film thickness is known, Eq. (17) is used to calculate the hydrodynamic friction force. Finally, Eq. (16) is employed to get the value for friction coefficient.

As presented in Sec. 4, the model has the ability to predict the gear performance when shear thinning lubricant is used. The corrections to the film thickness and hydrodynamic friction force are given in Eqs. (31) and (32).

In our simulation, the LoA is divided to 4000 points, and a typical execution time for this number of points is around 1 h on a Pentium 4 computer with a CPU of 1.8 GHz. The convergence criterion was chosen to be $\varepsilon=1\times10^{-5}$, meaning that when the right hand side of Eq. (29) minus the left hand side divided by the right hand side gets smaller than this number, the iteration will stop.

4 Results and Discussions

4.1 Verification Tests. The model was applied to a set of gear data and loading conditions that were obtained from literature [4] for verification purposes. Table 1 shows the geometrical properties and loading conditions of pinion and gear.

In Ref. [4] the lubricant was Newtonian and the surfaces were assumed to be smooth. For a comparison of current simulation and the original paper [4], the surface properties shown in Table 4 were selected to represent a very smooth surface [17]. It should be noted that surface properties are obtained from spectral moments of the surface, and they are not independent of each other.

Table 1 Pinion and gear data [4]

Number of pinion teeth	$z_p=28$
Number of gear teeth	$z_g=84$
Module	$m=0.003175$ m
Pinion pitch diameter	$d_{wp}=0.0889$ m
Pinion rotational speed	$\omega=1637$ rpm
Gear width	$B=0.1$ m
Load per unit width	$F=0.3765$ MN/m
Pressure angle	$\alpha=20$ deg
Oil viscosity	$\mu=0.065$ Pa s
Viscosity-pressure index	$Z=0.6$

The active length of LoA was divided to 4000 points, and the aforementioned calculations were done for each point. The variation of equivalent radius of curvature calculated from Eqs. (7)–(10) is shown in Fig. 3.

In the following figures, the abscissa is the coordinate along the LoA, i.e., the coordinate of the point on the pinion tooth that comes into contact. The negative part of the axis refers to pinion dedendum and the positive part refers to pinion addendum. Hence, the largest negative coordinate shows the beginning of mesh and the largest positive point refers to the end of mesh for the pinion tooth.

Figure 4 shows the variation of transmitted load along LoA. At the first point of contact (A), the transmitted load is shared by two pairs of teeth in contact until the contact point reaches point C. Thereafter, until the contact point reaches D, there is only one pair of tooth in contact. From point D to point B, there will, again, be two pairs of teeth in contact.

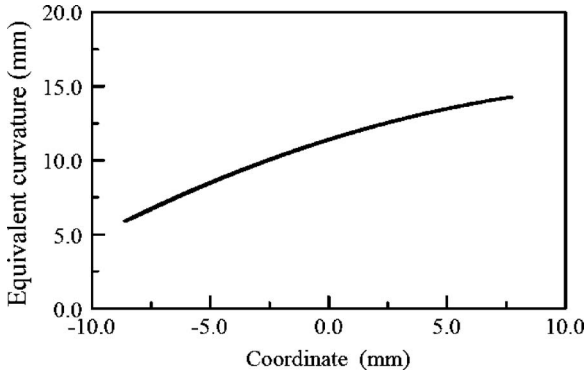

Fig. 3 Variation of equivalent radius of curvature along LoA

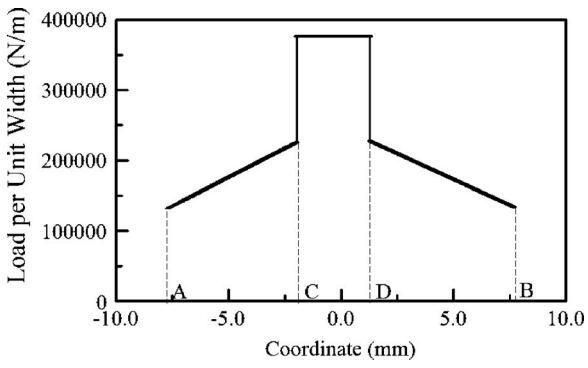

Fig. 4 Variation of load along LoA

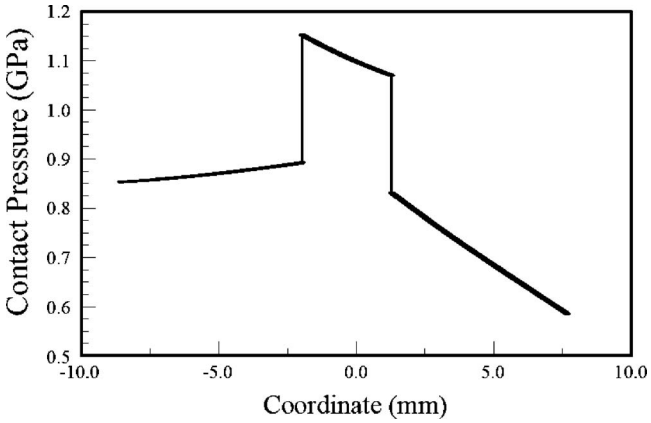

Fig. 5 Variation of contact stress along LoA

The variation of the Hertzian stress along LoA is shown in Fig. 5. The lowest point of single tooth contact experiences the largest contact stress.

The film thickness from the present simulation and the film thickness as calculated in Ref. [4] are shown in Fig. 6.

The film thickness comparison shows a good agreement between this model and the work of Hua and Khonsari [4], who solved the EHL problem by a direct solution of the Reynolds equation. The differences can be related to the fact that in Ref. [4] the surfaces were assumed to be perfectly smooth, but in our simulation the surface roughness is considered. Probably, that is why in pinion addendum, where the film thickness is larger and the effect of surface roughness becomes less pronounced, the results are closer. However, as shown in Table 2, the surface properties used for this comparison are selected such that the surface roughness is very small.

Next, we present simulation results corresponding to an experimentally measured friction coefficient. For this purpose, the experimental results of Lee [3] were selected. Lee's experiment was done with a twin disk machine. The test rig had a continually variable speed motor and a set of gears, which were used to provide different sets of roll to slide ratio. The experiment was designed for scuffing in heavily loaded EHL contacts, and as part of his experiment, Lee measured the friction coefficient. The test conditions of Lee's experiment are shown in Table 3.

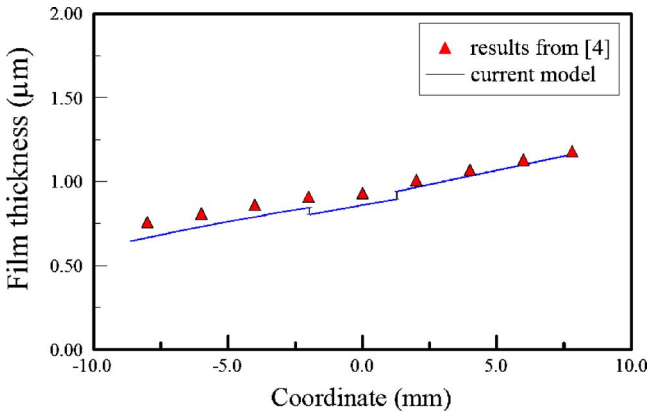

Fig. 6 Comparison of film thickness with results from Ref. [4]

Table 2 Surface properties [17]

RMS of the surface	$\sigma_s=0.05\ \mu$m
Density of asperity	$n=1.0\times10^{11}$ m^{-2}
Radius of asperity	$\beta=10.0\ \mu$m

Table 3 Test conditions [3]

Smaller roller radius	$R_p=13.97$ mm
Larger roller radius	$R_g=55.88$ mm
Width of the rollers	$b=25.4$ mm
Rolling velocity	$v_{roll}=3.83$ m/s
Sliding velocity	$v_{slide}=3$ m/s
Sliding to rolling ratio	$\Sigma=0.7826$
Oil viscosity at operating temperature	$\mu=0.063$ Pa s
rms of surface roughness	$\sigma_s=0.274\times10^{-6}$ m

The surface properties that are used in our model are shown in Table 4. The parameter σ_s is assumed to be exactly the same as the rms of surface roughness of the disks used in the experiment. The density of asperities and radius of asperity tip, however, are obtained from Ref. [17]. The coefficient of friction between asperities is a function of material and surface properties and is usually determined by experiments being conducted in the boundary lubrication regime between two rollers. For a wide range of surface properties from pretty smooth to fairly rough surfaces, the literature gives values from 0.10 to 0.13 for asperity friction coefficient. For this case, the variation from 0.1 to 0.13 for asperity friction coefficient will not influence the friction coefficient considerably, and almost the same accuracy will be maintained. The reason for this is the large contribution of fluid in taking the load.

Figure 7 shows the comparison between the present model and experiment for a range of loads.

The differences seen in the plot can be attributed to the manner in which the experiment was conducted. Initially, the rollers were pressed together with a force equal to 425 N. The test was run for 5 min, the friction coefficient and surface temperatures of the disks were collected, and then the normal load was increased, and the test continued for another 5 min. Our simulation is not a function of time and does not consider the effect of running in process.

4.2 Shear Thinning Simulations. Having verified the model for a Newtonian lubricant, next step is to check its validity for non-Newtonian lubricants such as shear thinning. These lubri-

Table 4 Surface properties [17]

Density of asperities	$n=1.25\times10^{10}$ (1/m^2)
Radius of asperity tip	$\beta=10\times10^{-6}$ m
rms of the surface	$\sigma_s=0.274\times10^{-6}$ m
Coefficient of friction between asperities	$f=0.1$

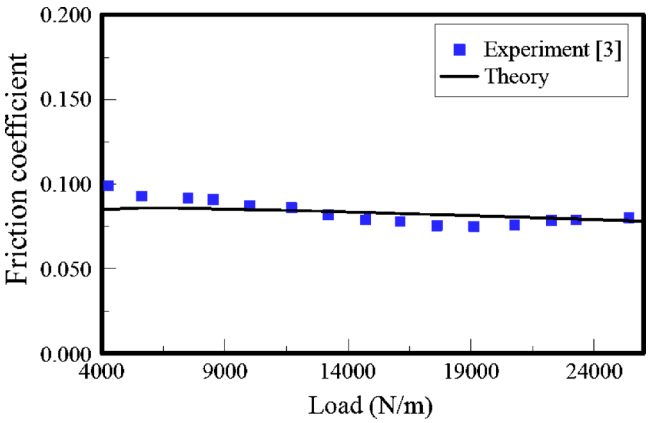

Fig. 7 Comparison of model results with experimental data [3]

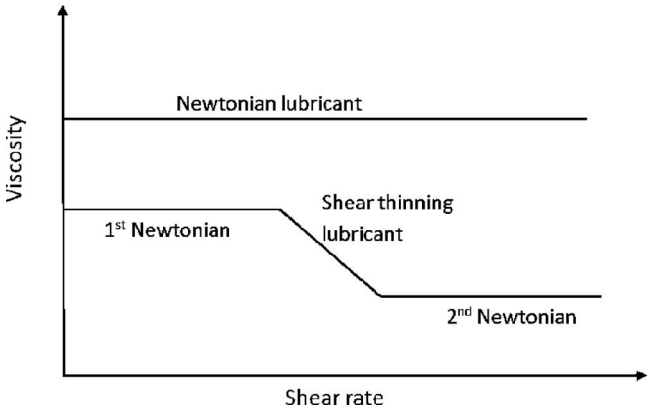

Fig. 8 Characteristics of shear thinning lubricant

cants, which are sometimes used by some industries, exhibit a shear thinning behavior, as illustrated in Fig. 8. At very low and very high shear rates, the lubricant behavior is the same fashion as a Newtonian fluid, and in the intermediate region it drops linearly with increase in shear rates.

In order to be able to predict the gear performance with shear thinning lubricant, some corrections have to be made. First, the film thickness needs to be modified. A correction factor called ϕ was proposed by Bair [11], which is the ratio of the Newtonian film thickness to the shear thinning film thickness. This factor is a function of the sliding to rolling ratio (Σ) and the Weissenberg number ($\Gamma = \mu_0 u / h_N G_C$), where u represents the rolling velocity, G_C denotes the critical stress, h_N is the film thickness by the Newtonian calculation, and μ_0 is the low-shear viscosity at ambient pressure,

$$\phi = \frac{h_N}{h_{NN}} = \{1 + 0.79[(1+\Sigma)\Gamma]^{1/1+0.2\Sigma}\}^{3.6(1-n)^{1.7}} \tag{30}$$

For a shear thinning lubricant, the hydrodynamic friction force $F_{f,H}$ is calculated using Carreau's equation [20],

$$F_{f,H} = 2Ba\dot{\gamma}\left\{\left[\mu_2 + (\mu_1 - \mu_2)\left(1 + \left(\frac{u_1\dot{\gamma}}{G_C}\right)^2\right)\right]^{(m-1)/2}\right\} \tag{31}$$

In this equation, μ_1 and μ_2 are the first and the second Newtonian viscosities, B is the width of the rollers, a is the half-width of contact, m is the power-law exponent, and $\dot{\gamma}$ is the shear rate and is defined as the ratio of the difference in speeds of the two rollers to the film thickness (h_c),

Table 5 Surface properties [19]

Density of asperities	$n = 3.31 \times 10^{10}$ (1/m^2)
Radius of asperity tip	$\beta = 6.02 \times 10^{-6}$ m
rms of the surface	$\sigma_s = 0.7 \times 10^{-6}$ m
Coefficient of friction between asperities	$f = 0.12$

$$\dot{\gamma} = \frac{u_1 - u_2}{h_c} \tag{32}$$

Figure 9 shows the film thickness for the shear thinning lubricant. For comparison, the Newtonian film thickness for the same case is plotted in the same figure. The geometry and loading conditions are the same as in Table 1. For this lubricant $m = 0.4$ and $G_c = 1 \times 10^6$ Pa, and the surface properties are derived from Table 5.

The results predict that the film thickness tends to increase along the LoA. In the region of single tooth contact, there is a higher contact stress, which results in a decrease in the film thickness. Around the pitch point when the effect of sliding becomes minor, the Newtonian and shear thinning film thicknesses become closer. Also, at the pitch point, there is a change in the slope of film thickness. This change is due to the behavior of the correction factor, which is a function of the slide/rolling ratio and the Weissenberg number. Figure 10 shows the variation of the Bair correction factor along the LoA.

As shown in Fig. 10, as the contact point moves toward the pitch point, sliding decreases and the value of the Bair correction factor ϕ decreases. As the contact point moves away from the pitch point, the correction factor increases.

4.3 Variation of Film Parameter and Surface Roughness. The dimensionless film parameter, which is the ratio of the film thickness to the surface roughness ($\Lambda = h_c / \sigma_s$), is of great importance in tribology. The variation of this parameter along the LoA is plotted in Fig. 11. The film parameter is a useful parameter for determining the severity of load and the lubrication regime. It is generally believed that $\Lambda < 1$ corresponds to boundary lubrication, whereas partial or mixed-film lubrication occurs when $1 < \Lambda < 3$ and for full elastohydrodynamic lubrication $\Lambda > 3$ [15]. According to Fig. 11, the lubrication regime for contact points in the pinion dedendum is boundary, while in pinion addendum it is mixed.

4.4 Friction Coefficient. Friction coefficient is a function of geometry, loading, and lubricant and determines the required torque (and power). Hence, this variable is a key parameter in the performance of a gear set. Figure 12 plots the variation of friction coefficient along the LoA for a Newtonian lubricant and a shear thinning lubricant. The input data, such as lubricant properties,

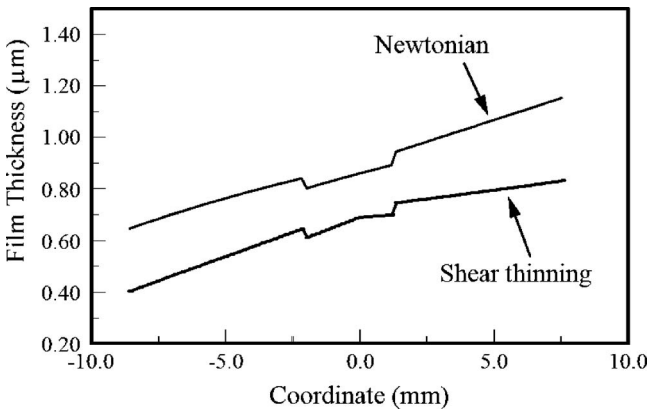

Fig. 9 Variation of film thickness along LoA

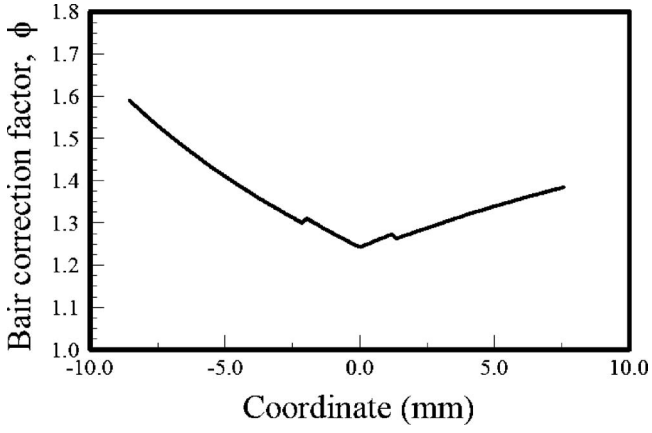

Fig. 10 Variation of ϕ along LoA

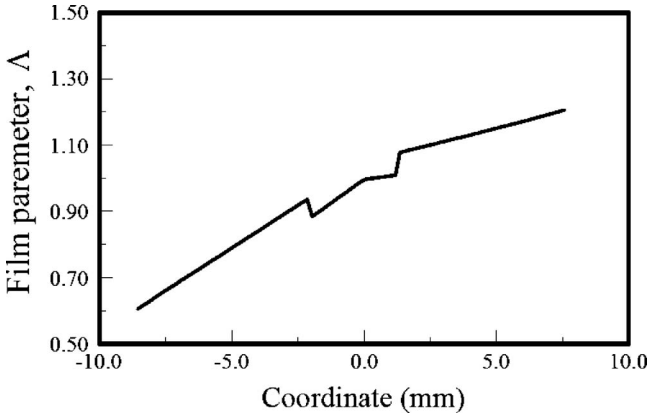

Fig. 11 Variation of film parameter (Λ) along LoA

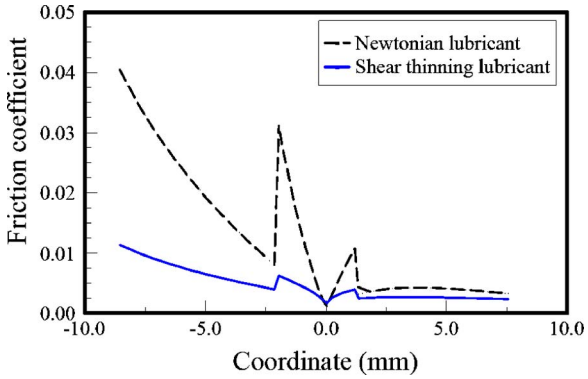

Fig. 13 Variation of friction coefficient along the LoA and comparison with Newtonian lubricant for $\sigma_s=0.4\times10^{-6}$ m

geometry, and loading, are taken from Table 1. For comparison, it was assumed that the first Newtonian viscosity for the shear thinning lubricant is the same as the viscosity of the other lubricant and that the second Newtonian viscosity is zero. For the Newtonian lubricant, the friction coefficient is highest at the first point of contact and drops as the contact point moves toward the pitch point and sliding decreases. At the lowest point of single tooth contact, there is a sudden increase in friction coefficient, which is due to the shift from two pairs of teeth to one pair of teeth in contact. At the pitch point, where there is pure rolling, the hydrodynamic friction force is zero and there is only asperity friction force. A sudden decrease is seen in the point of shift from one pair of teeth to two pairs of teeth in contact, and after that the friction coefficient remains almost constant. The shear thinning lubricant shows a similar behavior at points when the number of tooth in contact changes and also at the pitch point. This lubricant shows a smaller friction coefficient in comparison to the Newtonian lubricant.

To illustrate the effect of surface roughness on the performance of gear, the model was simulated for two other surface roughness parameters of $\sigma_s=0.4\times10^{-6}$ m and $\sigma=0.7\times10^{-6}$ m. The results are shown in Figs. 13 and 14. As shown in Fig. 13, the friction coefficient for both lubricants has a similar trend as in the smoother case (Fig. 12), except that there is a slight increase in the value of friction coefficient. This increase is due to the use of rougher surfaces; in this case, more asperities come into contact and they carry a larger portion of load.

Figure 14 compares the friction coefficient for even a rougher surface where $\sigma_s=0.7\times10^{-6}$ m. The value of the friction coefficient compared to the other two smoother cases is higher. For smoother cases, the asperity friction force is negligible, and most of the load is carried by the fluid film. When the surface becomes rough, the scaling factor for the asperity part becomes smaller, which means that more asperity contact will occur. Therefore, the asperity friction force will become the dominant part and the friction coefficient increases.

One of the outputs of the model is the scaling factors. That is, a percentage of load is taken by the fluid film and a percentage is taken by asperities. For the case in Fig. 14, the percentage of load taken by fluid film and asperities are shown in Fig. 15.

In the dedendum, the asperities take a larger portion of the load. As the contact point moves along the LoA, the film thickness

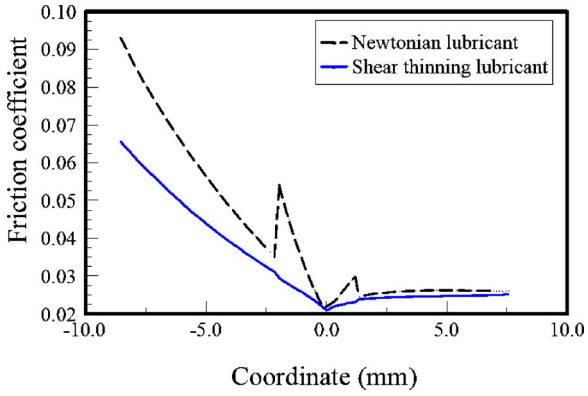

Fig. 14 Variation of friction coefficient along the LoA and comparison with Newtonian lubricant for $\sigma_s=0.7\times10^{-6}$ m

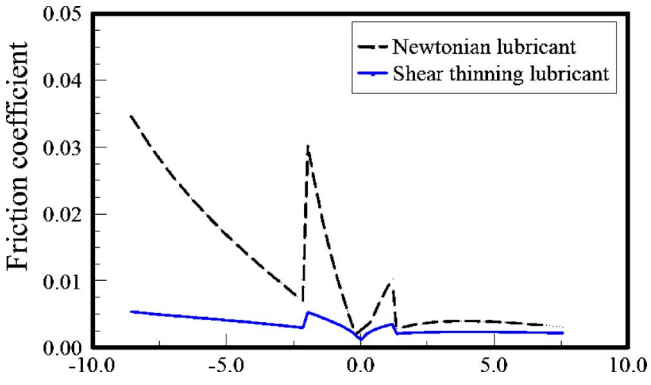

Fig. 12 Variation of friction coefficient along the LoA and comparison with Newtonian lubricant for $\sigma=0.1\times10^{-6}$ m

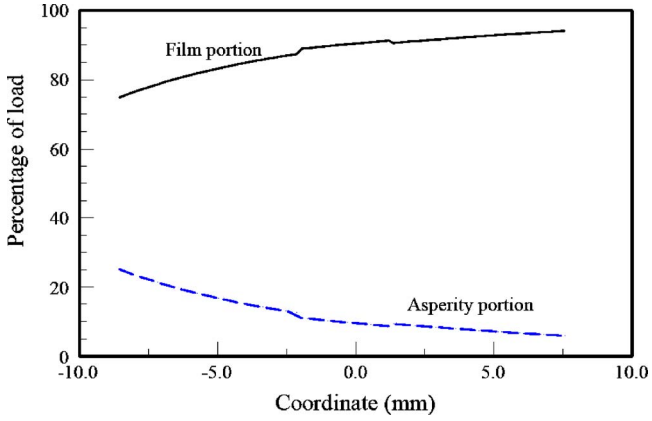

Fig. 15 Scaling factors along LoA for $\sigma_s=0.7\times10^{-6}$ m

increases and a larger portion of the load is carried by fluid film. The points of shift from two pairs of teeth to one pair of teeth can also be seen in Fig. 15.

5 Conclusions

In this paper, a useful approach for predicting the film thickness and friction coefficient of spur gears with consideration of surface roughness and provision for lubricant with shear thinning characteristic is reported. Either the asperity density, asperity radius, and rms of the surface are among the inputs to the model or the model calculates those using spectral moments of the surface. The model employs the concept of load sharing of Johnson et al. and applies Moes' equation for calculating the Newtonian central film thickness. The model can also be applied for non-Newtonian lubricants, such as shear thinning lubricants. In this case, the film thickness is corrected by using Bair's correction factor for shear thinning lubricants. Having calculated the film thickness, the model then uses Carreau's equation for calculating the hydrodynamic friction force. The main advantages of the model are that (i) the model does not require solving the full EHL equations, (ii) it generates reasonable results for rough surfaces, and (iii) the results are in acceptable agreement with experimental data. This model can be used as a rapid prediction for the gear performance since the code without need to solve the full EHL equations generates acceptable results.

Using the shear thinning lubricant instead of the Newtonian one will result in lower film thickness. At the beginning of contact, due to large sliding the film thickness is much smaller than the Newtonian film thickness. Around the pitch line where there is small sliding, the Newtonian and the shear thinning film thicknesses become closer.

The surface roughness obviously affects the friction coefficient. As the surface roughness increases, more asperities come into contact and a larger portion of the load is taken by asperities. Therefore, the friction coefficient will increase.

Comparing Newtonian and shear thinning lubricants indicates that a shear thinning lubricant shows a smaller friction coefficient. However, as the surface roughness increases, the difference between the friction coefficients of the two lubricants decreases. This decrease is due to the fact that for rougher surfaces, more asperities come into contact and carry a larger portion of the load. Hence, the asperity friction force becomes the dominant term.

Acknowledgment

This research was supported in part by a grant from Caterpillar Inc. to LSU Center for Rotating Machinery (CeRoM). The statements made in this paper are solely the opinions of the authors.

Nomenclature

a = half width of Hertzian contact, m
B = gear width, m
d_d = distance between mean line of asperities and mean line of surface, m
d_{wp} = pinion pitch diameter, m
E' = equivalent Young's modulus, N/m^2
F_T = transmitted force, N
F_H = load carried by fluid, N
F_C = load carried by asperity, N
$F_{f,H}$ = hydrodynamic friction force, N
$F_{f,C}$ = friction force from asperity interaction, N
f = coefficient of friction
f_c = friction coefficient between asperities
G_c = critical stress, Pa
h_c = central film thickness
h_N = Newtonian film thickness, m
h_{NN} = non-Newtonian film thickness, m
m = power-law exponent
n = density of asperities, $1/m^2$
R_p = radius of roller p, m
R_g = radius of roller g, m
u_{roll} = rolling velocity $(u_1+u_2)/2$, m/s
$u_{sliding}$ = sliding velocity, u_2-u_1, m/s
v = Poisson's ratio
z_p = number of pinion teeth
z_g = number of gear teeth
Z = viscosity-pressure index
α = pressure angle
α_{EHL} = pressure viscosity coefficient
β = average radius of asperities, m
γ_1 = scaling factor for hydrodynamic part
γ_2 = scaling factor for asperity contact part
Λ = film parameter
σ_s = standard deviation of asperities, m
Σ = slide to roll ratio, $2(u_1-u_2)/u_1+u_2$
ϕ = correction factor for shear thinning film thickness
ξ = coordinate along the LoA, m
ρ = radius of curvature of gears, m
ω = rotational speed, rpm

References

[1] Johnson, K. L., Greenwood, J. A., and Poon, S. Y., 1972, "A Simple Theory of Asperity Contact in Elastohydrodynamic Lubrication," Wear, **19**, pp. 91–108.
[2] Patir, N., and Cheng, H. S., 1978, "An Average Flow Model for Determining Effects of Three-Dimensional Roughness on Partial Hydrodynamic Lubrication," ASME J. Lubr. Technol., **100**, pp. 12–17.
[3] Lee, S., 1989, "Scuffing Modeling and Experiments for Heavily Loaded Elastohydrodynamic Lubrication Contacts," Ph.D. thesis, Northwestern University.
[4] Hua, D. Y., and Khonsari, M. M., 1995, "Application of Transient Elastohydrodynamic Lubrication Analysis for Gear Transmissions," Tribol. Trans., **38**, pp. 905–913.
[5] Chang, L., 1995, "A Deterministic Model for Line Contact Partial Elastohydrodynamic Lubrication," Tribol. Int., **28**, pp. 75–84.
[6] Flodin, A., and Andersson, S., 1997, "Simulation of Mild Wear in Spur Gears," Wear, **207**, pp. 16–23.
[7] Chapkov, A. D., Venner, C. H., and Lubrecht, A. A., 2006, "Roughness Amplitude Reduction Under Non-Newtonian EHD Lubrication Conditions," ASME J. Tribol., **128**, pp. 753–760.
[8] Khonsari, M. M., and Booser, E. R., 2001, *Applied Tribology Bearing Design and Lubrication*, Wiley, New York.
[9] Dyson, A., and Wilson, A. R., 1966, "Film Thickness in Elastohydrodynamic Lubrication by Silicone Fluids," Proc. Inst. Mech. Eng., **180**, pp. 97–105.
[10] Bair, S., and Khonsari, M. M., 2006, "Reynolds Equations for Common Generalized Newtonian Models and an Approximate Reynolds-Carreau Equation," Proc. Inst. Mech. Eng., Part J: J. Eng. Tribol., **220**, pp. 365–374.
[11] Bair, S., 2005, "Shear Thinning Correction for Rolling/Sliding Electrohydrodynamic Film Thickness," Proc. Inst. Mech. Eng., Part J: J. Eng. Tribol., **219**, pp. 1–6.
[12] Harris, T. A., 2001, *Rolling Bearing Analysis*, Wiley, New York.
[13] Wang, K. L., and Cheng, H. S., 1981, "A Numerical Solution to the Dynamic Load, Film Thickness and Surface Temperature in Spur Gears, Part I Analysis," ASME J. Mech. Des., **103**, pp. 177–187.
[14] Errichello, R., 1992, "Friction, Lubrication, and Wear of Gears," *ASM Handbook*, CRC Press, Boca Raton, FL, Vol. 18, pp. 535–545.
[15] Hamrock, B. J., 1994, *Fundamentals of Fluid Film Lubrication*, McGraw-Hill, New York.
[16] Moes, H., 1992, "Optimum Similarity Analysis With Applications to Elastohydrodynamic Lubrication," Wear, **159**, pp. 57–66.
[17] Gelinck, E. R. M., and Schipper, D. J., 2000, "Calculation of Stribeck Curves for Line Contacts," Tribol. Int., **33**, pp. 175–181.
[18] Prakash, J., and Czichos, H., 1983, "Influence of Surface Roughness and Its Orientation on Partial Elastohydrodynamic Lubrication of Rollers," ASME J. Lubr. Technol., **105**, pp. 591–597.
[19] Lu, X., Khonsari, M. M., and Gelinck, E. R. M., 2006, "The Stribeck Curve: Experimental Results and Theoretical Prediction," ASME J. Tribol., **128**, pp. 789–794.
[20] Carreau, P. J., 1972, "Rheological Equations From Molecular Network Theories," Trans. Soc. Rheol., **16**, pp. 99–127.